A detonation run-up distance database: data-driven existing models improvement and new model development

Cristian Mejía-Botero, Florent Virot, Luís Fernando Figueira da Silva, J. Melguizo-Gavilanes

A detonation run-up distance database: data-driven existing models improvement and new model development

C. Mejía-Botero[a,*], F. Virot[a], L.F. Figueira da Silva[a], J. Melguizo-Gavilanes[a,b]

[a] *Institut Pprime, CNRS, ISAE–ENSMA, Université de Poitiers, BP 40109, 86961 Futuroscope–Chasseneuil Cedex, France*
[b] *Shell Global Solutions B.V., Major Hazards Management, Energy Transition Campus, 1031 HW Amsterdam, The Netherlands*

Abstract

A comprehensive database of detonation run-up distances (x_{DDT}) in unobstructed tubes/channels is compiled. Eight fuels are included, i.e., hydrogen, methane, ethane, ethylene, acetylene, propane, butane and carbon monoxide. Oxygen is used as oxidizer with different diluents under a wide range of tube/channel sizes. In total 559 points are collected and analyzed. The global x_{DDT} trends observed in the data as a function of the initial conditions (i.e., fuel type, equivalence ratio (ϕ), hydraulic diameter (D_{h}), and pressure (p)) reveal that x_{DDT} decreases with increasing p, decreasing D_{h}, and $\phi \rightarrow 1$. The correlation of the normalized run-up distance $x_{\mathrm{DDT}}/D_{\mathrm{h}}$ with geometrical parameters and fundamental combustion properties shows that most of the variance in the experimental data can be captured by the ratio of D_{h} to the flame thickness ($D_{\mathrm{h}}/\delta_{\mathrm{f}}$), the expansion ratio ($\sigma - 1$) and that of the Chapman-Jouguet to the laminar flame speed ($V_{\mathrm{CJ}}/\sigma s_{\mathrm{L}}$). With these, a non-linear (NLM) and a logarithmic model (LM) are proposed using a non-linear least squares regression to fit a user-defined function. The NLM and LM are shown to outperform the widely used Silvestrini and Dorofeev models by a large margin since they are capable of explaining $\sim 70 - 80\%$ of the variance in the experimental $x_{\mathrm{DDT}}/D_{\mathrm{h}}$ data in contrast to only $\sim 20\%$ of the original Silvestrini and Dorofeev models. The poor performance of the original models is due to the limited amount of data used to determine the models constants. An update to these constants is also carried out using the database collected in this work resulting in a notable improvement of their predictive capabilities over the original models. The database is publicly available so that it can be used freely to guide future research in the combustion community (e.g., by identifying conditions where there is a lack of data), and as a test bed for further data-driven model development.

Keywords: Deflagration-to-detonation transition; detonation run-up distances; data-driven models; flame acceleration; fuel safety

Information for Colloquium Chairs and Cochairs, Editors, and Reviewers

1) Novelty and Significance Statement

The novelty of this research is the compilation of large detonation run-up distance, x_{DDT} database comprising 559 data points for 8 fuels under a wide range of experimental conditions, i.e., hydraulic channels/tubes diameters ($0.5 \leq D_{\mathrm{h}} \leq 406$ mm), equivalence ratios ($0.2 \leq \phi \leq 5.8$), diluents (N_2, Ar, He, CO_2), initial pressure ($0.1 \leq p \leq 25$ bar), and temperature ($298 \leq T \leq 473$ K). It is significant because with this database two data-driven models were developed capable of explaining $\sim 70-80\%$ of the variance in the experimental $x_{\mathrm{DDT}}/D_{\mathrm{h}}$ data in contrast to only $\sim 20\%$ that the most widely used correlations currently capture (e.g., Silvestrini and Dorofeev). This constitutes a sizeable advancement over the state of the art. Moreover, the database is freely available to the combustion community so that anyone can exploit the synergies between physics-based reasoning and data-driven learning.

2) Author Contributions

- **C. Mejía-Botero:** performed the research, analyzed data, wrote the paper
- **F. Virot:** analyzed data, reviewed & edited.
- **L.F. Figueira da Silva:** analyzed data, reviewed & edited.
- **J. Melguizo-Gavilanes:** designed the research, analyzed data, wrote the paper, reviewed & edited.

3) Authors' Preference and Justification for Mode of Presentation at the Symposium

The authors prefer **OPP** presentation at the Symposium, for the following reasons:

- The subject is approached originally and the focus is placed on outcomes and results
- Our contribution is expected to prompt/benefit from fruitful room-audience-level discussions
- An extensive database (559 points) for x_{DDT} in unobstructed channels is compiled
- The most widely-used correlations for x_{DDT} predictions are shown to perform poorly against our database
- Well-known models are challenged and 2 data-driven alternatives that capture $70-80\%$ of the experimental variance are proposed

1. Introduction

Under certain conditions, after accidental ignition of a reactive cloud, the initial flame may accelerate and transit to detonation, the so-called, deflagration-to-detonation-transition (DDT) phenomenon. Detonation is a supersonic combustion propagation regime that is much stronger and more destructive than a flame. Although in most cases DDT occurs due to flame/shock/obstacles interactions, it can also occur in unobstructed spaces, such as gas compartments and hoses in fuel cells, battery packs, electrolyzers, among others. The DDT run-up distance, x_{DDT}, is the distance between the ignition of the flame and the onset of detonation. The determination of x_{DDT} is not only important for safety but also for the optimal design of pulse detonation engines (PDE) [1].

One way to estimate x_{DDT} is using experimental data together with phenomenological models. For the latter, those proposed by Silvestrini et al. [2] and Dorofeev et al. [3] are the most widely used for predicting x_{DDT} in unobstructed channels. In [2] an expression for $x_{\text{DDT}}/D_{\text{h}}$ is proposed, where D_{h} is the hydraulic diameter of the tube/channel; hereinafter, the word channel(s) will be used to refer to either. The model assumes that the flame: (i) is ignited at the closed end and propagates towards the open end; (ii) its speed, V_{F}, increases exponentially with the relative axial position of the channel, x/D_{h}, i.e., $V_{\text{F}} = \text{A}\sigma s_{\text{L}} \exp\left[\text{B}(\sigma-1)(x/D_{\text{h}})(D_{\text{h}}/D_{\text{ref}})^n\right]$, where s_{L} is the laminar flame speed, σ is the expansion ratio, D_{ref} is a reference diameter, and A, B, and n are constants.

To estimate the constants, six $V_{\text{F}}(x)$ experimental data for hydrogen (H_2), propane (C_3H_8), and ethylene (C_2H_4) in air [4, 5] were used. These tests were performed in 150, 250, and 1400 mm diameter channels. Only one $V_{\text{F}}(x)$ profile per mixture was considered during curve fitting. The criterion to predict $x_{\text{DDT}}/D_{\text{h}}$ is that V_{F} must achieve a critical value suitable to trigger the DDT, that is, half of the Chapman–Jouguet detonation velocity, $V_{\text{F}} = V_{\text{CJ}}/2$. Silvestrini's model is thus

$$\frac{x_{\text{DDT}}}{D_{\text{h}}} = \frac{1}{B(\sigma-1)}\left(\frac{D_{\text{ref}}}{D_{\text{h}}}\right)^n \ln\left(F\frac{V_{\text{CJ}}}{\sigma s_{\text{L}}}\right), \quad (1)$$

where $B = 0.0061$, $n = 0.4$, $D_{\text{ref}} = 0.15$ m, and $F = 0.5/A = 0.077$. Since the constants were not determined directly using x_{DDT} data but with $V_{\text{F}} = f(x)$ profiles, the model prediction is limited by the $V_{\text{F}} = V_{\text{CJ}}/2$ assumption.

On the other hand, the model proposed in [3] is derived via a mass balance considering that the flame propagation speed is affected by the hydrodynamic boundary layer (BL) growth in the tube/channel whose relative thickness is denoted by Δ. To estimate Δ, the BL is assumed to grow linearly with the tube's wall roughness, d and axial position, x, i.e., $x/\Delta = [\ln(\Delta/d)/\kappa + K]/C$, where C, κ and K are constants. $x_{\text{DDT}}/D_{\text{h}}$ is obtained upon substitution of the latter expression into the mass balance, and assuming that DDT occurs when V_{F} reaches the sound speed in burnt gases, i.e., $V_{\text{F}} = c_{\text{b}}$. Dorofeev's model is

$$\frac{x_{\text{DDT}}}{D_{\text{h}}} = \frac{\Gamma}{C}\left[\frac{1}{\kappa}\ln\left(\Gamma\frac{D_{\text{h}}}{d}\right) + K\right], \quad (2)$$

$$\text{where} \quad \Gamma = \left[\frac{c_{\text{b}}}{\zeta(\sigma-1)^2 s_{\text{L}}}\left(\frac{\delta_{\text{f}}}{D_{\text{h}}}\right)^{\xi}\right]^{\frac{1}{2m+7/3}},$$

and $\delta_{\text{f}} = \alpha/s_{\text{L}}$ is the laminar flame thickness with α denoting the mixture thermal diffusivity; ζ and m are additional constants. To estimate the constants, $V_{\text{F}}(x)$ data from [6–10] were used. A total of nine tests, eight for H_2-O_2/air mixtures and only one for hydrocarbons (HC). Four of these were performed using channels with blockage ratio ≈ 0.1, which is known to modify the DDT behavior compared with unobstructed channels. The D_{h} range considered was $D_{\text{h}} \in [15, 520]$ mm resulting in $C = 0.2, \kappa = 0.4, K = 5.5, \zeta = 2.1, \xi = 1/3$ and $m = -0.18$.

It is evident that the models performance hinges on the appropriate determination of the constants. The limited data used in [2] and [3] did not consider a wide range of fuels, diluents, compositions/equivalence ratios (ϕ) and D_{h}, so their predictions are expectedtly restricted. Indeed in [11], Silvestrini's model was evaluated against data from [12, 13] showing poor performance for all the experimental conditions tested. For DDT predictions, large amounts of data are required to account for the randomness/variability of the process.

To fill this gap, here, a large database is compiled using all the x_{DDT} data for unobstructed channels available in the literature. In total, 559 tests were collected, including both HCs and H_2 over a wide range of experimental conditions (D_{h}, ϕ, pressure (p) and temperature (T)). The constants of the Silvestrini and Dorofeev models are updated resulting in a significant improvement of their predictive capabilities. Furthermore, two additional simpler expressions that outperform the original Silvestrini and Dorofeev models by a large margin are proposed.

2. Database description

To collect the data a systematic search was performed in *Scopus*. As criteria, only scientific papers reporting experimental x_{DDT} values obtained in unobstructed channels using weak ignition sources to avoid direct detonation initiation were considered. x_{DDT} is compiled together with the mixture initial conditions, i.e., T, p, and ϕ. Geometrical information such as D_{h}, length (L), cross-section (CS) and boundary conditions (BC) are also included. The latter refers to channels with Closed/Closed (C/C) or Closed/Opened ends (C/O). Table 1 summarizes the data collected. A total of 36 references were reviewed. The data are split into C/O and C/C chan-

nels, and ordered according to the fuel used. Experimental data obtained for the current work in the two-directional schlieren visualization set-up described in [14, 15] are included as well.

2.1. Geometrical parameters

The ranges of L and D_h for which data were found are $L \in [0.4, 40]$ m and $D_\mathrm{h} \in [0.6, 406]$ mm, and $L \in [0.8, 24]$ m and $D_\mathrm{h} \in [0.5, 159]$ mm for C/O and C/C channels, respectively. The minimum and maximum L/D_h ratios in the dataset are $L/D_\mathrm{h} = 6$ and 4000.

2.2. Mixtures and initial conditions

A total of eight fuels are included, i.e., H_2, methane (CH_4) ethane (C_2H_6), C_2H_4, acetylene (C_2H_2), C_3H_8, butane (C_4H_{10}) and carbon monoxide (CO). Almost all are fuels of a single component, except for some in [30] that correspond to CH_4/C_2H_6, some in [26] that used H_2/C_3H_8, and some measured by the current authors using H_2/CH_4 blends. Oxygen (O_2) is the oxidizer. Nitrogen (N_2), helium (He), argon (Ar) and carbon dioxide (CO_2) are used as diluents. The initial conditions ranges are $T \in [298, 473]$ K, $p \in [0.1, 25]$ bar, and $\phi \in [0.2, 5.8]$.

2.3. Number of data points and distribution

Table 1 also shows the number of data points (DP) per fuel. 202 and 357 DP were collected for C/O and C/C which correspond to a total of 559 tests. H_2 and C_2H_4 are the most often used fuels, with 193 and 191 DP, respectively. These are followed by C_3H_8 (95 DP), and CH_4 (29 DP). The less used are C_2H_2 (18), CO (15 DP), C_2H_6 (9 DP), and C_4H_{10} (9 DP).

Figure 1 shows the D_h, Φ and p histograms for (a) C/C, and (b) C/O. Tests carried out with H_2 and HC are plotted with different colors; the 15 DP with CO are not included. The histograms reveal that for both BCs most of the tests were performed in channels with $D_\mathrm{h} \leq 50$ mm.

Regarding mixture compositions, the normalized equivalence ratio, $\Phi = \phi/(1+\phi)$ is used to center the distribution at $\phi = 1.0$ (i.e., $\Phi = 0.5$). For C/O, most of the tests are performed with HC fuels of which 81 DP correspond to stoichiometric ($\Phi = 0.5$), 28 to lean ($\Phi < 0.5$), and 37 to rich ($\Phi > 0.5$) conditions. For H_2, 29 DP correspond to $\Phi = 0.5$, 11 to $\Phi < 0.5$, and 16 to $\Phi > 0.5$. For C/C, the data is distributed as follows: 171 DP at $\Phi = 0.5$, 14 at $\Phi < 0.5$, and 20 at $\Phi > 0.5$ for HC mixtures. For H_2 mixtures, 81 DP correspond to $\Phi = 0.5$, 29 to $\Phi < 0.5$, and 27 to $\Phi > 0.5$. Finally, the p histogram shows, expectedly, that all the tests with C/O channels are performed at atmospheric pressure, i.e., $p \approx 1$ bar. For C/C, most of the tests are carried out at $p < 1$ bar with 157 and 14 DP for HC and H_2 mixtures, respectively. For $p > 1.0$ bar, 21 (HC) and 92 (H_2) DP were found, and at $p = 1.0$ bar, 27 (HC) and 31 (H_2) DP were collected

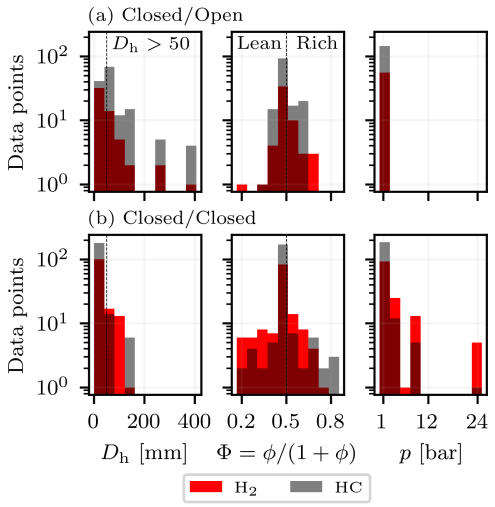

Fig. 1: Histograms for D_h, Φ and p. (a) Closed/Open; (b) Closed/Closed channels.

A key advantage of this visualization is that it permits to identify regions where there is little to no data available in the literature. This may serve as a guide for future DDT research. As an example, only 9 data points were collected at 473 K for C/C channels [22]. The remaining of the data were obtained at room temperature, i.e., $\approx$ 298 K. This shows high research potential of the effect of T on x_DDT in unobstructed channels since most of the industrial processes where DDT may occur are either at high T, e.g., electrolyzers and nuclear reactors, or low T, e.g., cryogenic fuel or oxidizer transportation. Additionally, the lack of data for $D_\mathrm{h} > 50$ mm is evident, which corresponds to most of the industrial pipelines in service. Data is missing for C_2H_2, C_2H_6, and C_4H_{10}, HC extensively used in many industries. Likewise for CO, of interest because it is one of the main components of Syngas which is expected to play an important role in the energy transition. Finally, note that most data exist at stoichiometric conditions but many accidents are the result of accidental ignition of a reactive cloud after leakage/mixing of fuel/oxidizer effectively resulting in scenarios where lean/rich mixtures are present.

2.4. Preprocessing of database

Three conditions were identified for which the DP follow different trends compared to most of the tests in the database: (i) channels with $D_\mathrm{h} < 3$ mm; 123 DP from [23–25, 33–35, 41, 42]. These include tests with both H_2 and HC for C/O and C/C at $\phi \in [0.7, 1.7]$, and $p \in [0.1, 2.4]$ bar performed mostly in spiral channels or with central ignition. (ii) channels with non-unity aspect ratio (AR); 119 DP from [27, 36] with AR ranging from 1:1.5 to

Table 1: Database summary.

Fuel	BC	ϕ	Diluents	D_h [mm]	L [m]	p [bar]	CS	DP	References
H_2	C/O	$0.25-2.1$	N_2, Ar, He	$3-406$	$1-40$	1	Cir.; Sqr.	56	[5, 11, 12, 14, 16–21], CW
	C/C	$0.2-2.8$	N_2, Ar, He, CO_2	$0.5-159$	$0.8-24$	$0.1-25$	Cir.; Rec.	137	[6, 7, 13, 22–29]
CH_4	C/O	1.0	N_2	$10-50$	$1-11$	1	Cir.; Sqr.	12	[11, 15, 18, 30], CW
	C/C	$0.35-2.0$	N_2	$15-20$	$1.5-2.9$	$0.3-25$	Cir.; Sqr.	17	[22, 31]
C_2H_2	C/O	–	–	–	–	–	–	–	–
	C/C	$0.27-5.8$	N_2	15	2.9	$1-5$	Cir.	18	[22]
C_2H_4	C/O	$0.63-1.7$	N_2	$0.6-406$	$0.4-40$	1	Cir.; Sqr.	55	[5, 11, 18, 32–35]
	C/C	$0.35-2.7$	N_2	$10-127$	$1-6$	$0.1-1.7$	Cir.; Rec.	136	[7, 28, 36–39]
C_2H_6	C/O	1.0	N_2	$26-50$	$2-11$	1	Cir.	9	[18, 30]
	C/C	–	–	–	–	–	–	–	–
C_3H_8	C/O	$0.5-1.7$	N_2	$25.4-406$	$0.5-40$	1	Cir.	61	[5, 11, 30, 32, 40]
	C/C	1.0	N_2	$0.5-3$	2	$0.1-1$	Cir.	34	[26, 41]
C_4H_{10}	C/O	1.0	N_2	50.8	11	1	Cir.	9	[30]
	C/C	–	–	–	–	–	–	–	–
CO	C/O	–	–	–	–	–	–	–	–
	C/C	$0.4-2.0$	–	50	2.9	$5-25$	Cir.	15	[22]

Legend: current work (CW); circular (Cir.); square (Sqr.); rectangular (Rec.). Refs. [27, 36] include channels with AR $\neq 1$.

1:30. These include tests with stoichiometric H_2 and C_2H_4 at $p < 0.7$ bar. (iii) the use of CO as fuel, with 15 DP from [22]; these tests were carried out at high pressure, i.e., $p \in [5-25]$ bar. Only data that did not meet the conditions above are considered in the analysis that follows. A total of 302 DP are thus retained after filtering: 132 for H_2 and 170 for HC mixtures. The final experimental ranges are $D_h \in [3, 406]$ mm, $\phi \in [0.2, 5.8]$, $p \in [0.12, 25]$ bar, and $T \in [298, 474]$ K.

The database and scripts will be made publicly available as a github repository.

3. x_{DDT} trends

3.1. x_{DDT} vs. D_h, Φ, and p

It is of practical interest (safety/propulsion) to identify/verify the general dependence of x_{DDT} on geometrical and initial conditions. Figure 2 shows these trends as a function of D_h, Φ, and p. For ease of visualization, selected cases were taken from the database to isolate the effect of the respective variable on x_{DDT}, however, the trends hold for all mixtures considered. Concerning D_h, stoichiometric ($\Phi = 0.5$) H_2/air and C_2H_4/air at $p = 1$ bar from [5, 16, 32]. The plot shows that x_{DDT} increases almost linearly with D_h for both mixtures. Regarding Φ, H_2/air and C_3H_8/air mixtures from [16, 32] tested in $D_h = 50$ mm channels at $p = 1$ bar. A U-shape curve is observed with x_{DDT} exhibiting a minimum around $\Phi = 0.5$. Finally for p, part of the experiments presented in [22] for H_2/O_2 and CH_4/O_2 in $D_h = 15$ mm channels at $\Phi = 0.5$ are shown. There is a pronounced decrease in x_{DDT} as p increases. The trends reveal that HC-air always lead to longer x_{DDT} compared to H_2-air. Conversely, the use of pure O_2 as oxidizer significantly decreases x_{DDT} for both types of mixtures. Based on the database collected, for PDE design where short x_{DDT} values are desirable, small D_h channels at high pressure and under stoichiometric conditions using pure O_2 as oxidizer are advised; the opposite holds for safety applications.

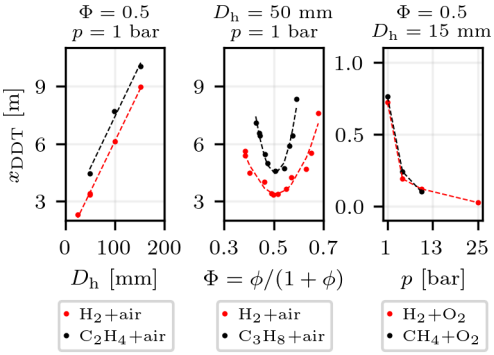

Fig. 2: x_{DDT} trends vs. D_h, Φ, and p for selected cases.

3.2. x_{DDT}/D_h vs. fundamental combustion properties

The effect on x_{DDT} of the (ratios of) fundamental combustion properties (i.e., $V_{CJ}/\sigma s_L$, c_b/s_L, and $\sigma - 1$) and that of the channel size to the laminar flame thickness (i.e., D_h/δ_f) used in the Silvestrini and Dorofeev models is evaluated next to assess whether the dependencies assumed hold, and to identify potentially overlooked relevant variables. The analysis is carried out on x_{DDT}/D_h to absorb channel size effects

on the output variable. The hydraulic diameter to detonation induction length ratio, D_h/l_{ind}, the Zel'dovich number, $\beta = E_a(T_b - T_u)/(RT_b^2)$, and the heat capacity ratio, $\gamma = c_p/c_v$, are also evaluated. E_a is the effective activation energy, T_b and T_u are the burnt and unburnt/fresh gases temperature, respectively; c_p and c_v are the heat capacity at constant pressure and volume. All properties were computed with Cantera using GRI 3.0 chemical mechanism, except for C_4H_{10} for which the San Diego mechanism was used. Figure 3 shows the Pearson autocorrelation matrix for the properties considered which measures colinearity between two sets of data. Values close to unity indicate a strong correlation, and suggest that these variables capture the x_{DDT}/D_h dependencies observed in the data.

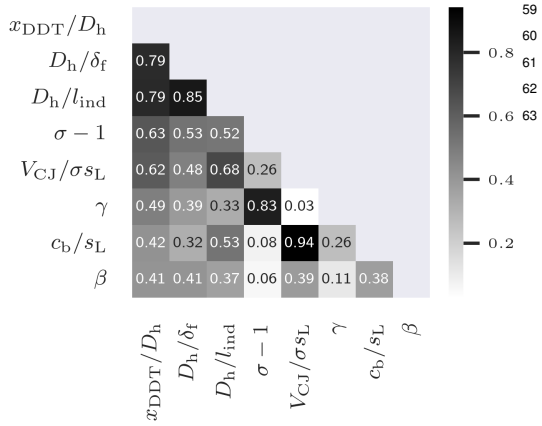

Fig. 3: Pearson autocorrelation matrix for x_{DDT}/D_h.

The most correlated with x_{DDT}/D_h are D_h/δ_f and D_h/l_{ind}, both with correlation coefficients of 0.79. Note however that these two variables are also correlated with each other indicating that they provide similar statistical information about x_{DDT}/D_h. D_h/δ_f is retained since for flame propagation and acceleration δ_f is a more sensible length scale to consider. Notably, the latter ratio is included in Dorofeev's and not in Silvestrini's model. The next in line is $\sigma - 1$ which was found to have a strong effect on the x_{DDT}/D_h predictions that will be presented in section 5, and to be highly correlated to γ; both Silvestrini and Dorofeev include $\sigma - 1$ and omit γ in their models. The following is $V_{CJ}/\sigma s_L$ (used in Silvestrini) which in turn is correlated to c_b/s_L (used in Dorofeev). The former ratio is retained because of its higher correlation with x_{DDT}/D_h. Finally, β exhibits a correlation coefficient of 0.41. While similar to that of c_b/s_L, it does not seem to be correlated to any of the other variables considered. The addition of this property to the models proposed in section 5 had a very modest effect on their performance, consequently, it was not considered further.

Figure 4 shows the trends of x_{DDT}/D_h with D_h/δ_f, $V_{CJ}/\sigma s_L$, and $\sigma - 1$. The BC type does not seem to have an important effect on x_{DDT}/D_h since both C/O and C/C follow the same behavior. D_h/δ_f is inversely proportional to x_{DDT}/D_h. Large D_h/δ_f values indicate that the flame is thin compared to the tube/channel dimensions, which in turn favors the development of surface instabilities and large flame surface area. This results in increased flame acceleration leading to a decrease in x_{DDT}/D_h. On the other hand, x_{DDT}/D_h is directly proportional to $V_{CJ}/\sigma s_L$. A mixture with high V_{CJ} must be accelerated more prior to transition, and a low σs_L is representative of mixtures with slow laminar flame speeds. It is thus expected that a large $V_{CJ}/\sigma s_L$ ratio results in large x_{DDT}/D_h values. Finally, of interest is that $\sigma - 1$, exhibits different slopes for H_2 and HC while both being inversely proportional to x_{DDT}/D_h. The latter observation stems from the fact that there is a large difference in σ between both fuel types. For the conditions of interest (i.e., flame acceleration in channels ignited at the closed end), higher σ values lead to increased acceleration rates during the early stages of flame propagation.

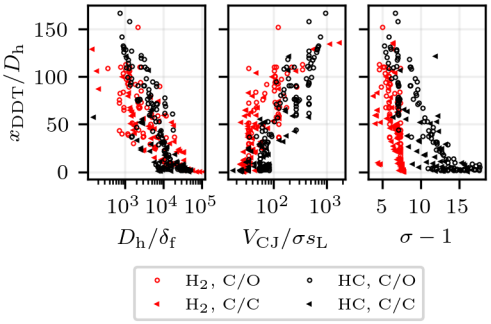

Fig. 4: x_{DDT}/D_h vs. ratios of fundamental combustion properties.

4. Existing model evaluation

4.1. Silvestrini and Dorofeev vs. database

Figure 5 compares the models predictions against the experimental database. A 45° line showing the ideal performance is added as a visual aid. That is, values that are predicted well by the models are expected to fall on this line. Most references do not report the standard deviation of their x_{DDT} data, hence an arbitrarily defined deviation band of $\pm 15\%$ is plotted to account for experimental uncertainties. The coefficient of determination (R^2) is used as our metric to assess the models performance. It was computed using standard functions from the scikit-learn package [43]. The best possible score is $R^2 = 1$ and it can be negative. A negative R^2 implies that a model fits the data worse than a horizontal line at a height equal to the mean of the observed data. This occurs when a wrong model is chosen or nonsensical constraints are inadvertently applied.

Both models performed poorly with R^2 of -0.88 and 0.23 for Silvestrini and Dorofeev, respectively. R^2 was also computed for H_2 and HC mixtures separately. The scatter is higher for H_2 mixtures ($R^2_{H2} = -3.5$ (Silvestrini) and -0.05 (Dorofeev)) than with HCs ($R^2_{HC} = 0.54$ (Silvestrini) and 0.37 (Dorofeev)).

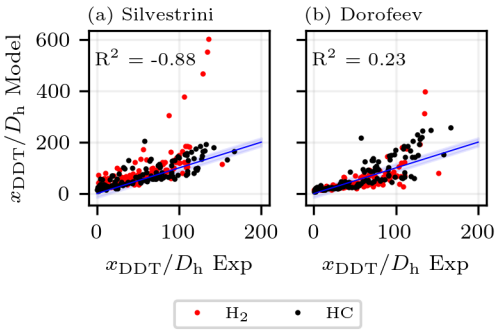

Fig. 5: Original models performance against database: a) Silvestrini and b) Dorofeev.

4.2. Updated Silvestrini and Dorofeev constants

An update to Silvestrini and Dorofeev model constants was done using the database collected in this work which includes a much wider range of operating conditions and fuels. As the fitting target is x_{DDT} rather than $V_F = f(x)$ data, it allows for a direct prediction/estimate of the variable of interest. 80 % of the data were used as the training set and 20 % as the test set. That is, 242 DP were used to determine the constants and 60 DP to evaluate the performance of the models. To select these data, the $train\_test\_split()$ function of scikit-learn [43] was used. It splits the data randomly by selecting a user-defined percentage. The initial conditions ranges for the training data are $D_h \in [3, 406]$ mm, $\phi \in [0.2, 5.8]$, $p \in [0.12, 25]$ bar, and $T \in [298, 474]$ K, and for the test data $D_h \in [3, 406]$ mm, $\phi \in [0.21, 2.8]$, $p \in [0.21, 25]$ bar, and $T \in [298, 474]$ K. The fitting was carried out using the $optimize.curve\_fit()$ function of SciPy which essentially uses a non-linear least squares regression method to fit a function. The updated constants are listed in Table 2.

Figure 6 shows the fitting results with the training data and the performance with the test data for the updated a) Silvestrini, and b) Dorofeev. The improvement is evident with R^2 values of 0.74 and 0.73 for the respective models. Their performance with the test data have R^2 of 0.7 and 0.71, respectively. Again, this represents significant improvements compared to the original models, and indicates that $\sim$ 70% of the variance in x_{DDT}/D_h can now be explained by the updated models. The remaining $\sim$ 30% can be attributed to unknown lurking variables or inherent variability. Note that the model's underlying assumptions were carefully verified to ensure that the updated constants values did not lead to non-physical flame velocities (Silvestrini) or unreasonable BL growth (Dorofeev) as a function of the axial position in the channel. Silvestrini/Dorofeev resulted in a measurable/modest increase/decrease compared to that originally obtained. The revised $V_F(x)$ and $\Delta(x)$ dependence better reflects the experimentally observed trends (not shown).

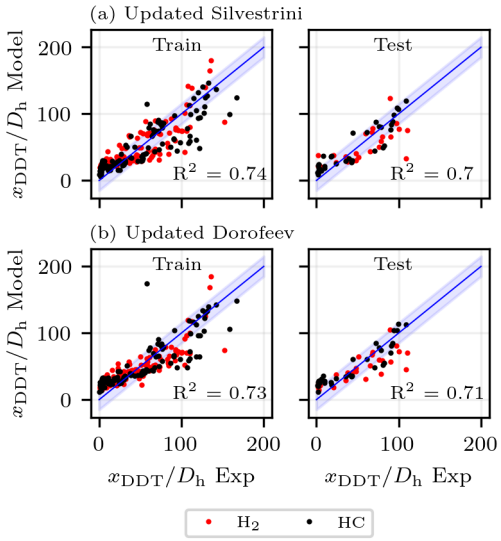

Fig. 6: Updated a) Silvestrini and b) Dorofeev performance for training and test data.

5. Proposed models

Two additional simpler models are proposed, i.e., non-linear (NLM) and logarithmic (LM), that leverage the learnings from the data analysis carried out in the previous sections. The expressions are shown in Equation 3, and Equation 4, respectively.

$$\frac{x_{DDT}}{D_h} = \frac{a_0}{(\sigma-1)^{a_1}} \left(\frac{D_h}{\delta_f}\right)^{-a_2} \left(\frac{V_{CJ}}{\sigma s_L}\right)^{a_3}, \quad (3)$$

$$\frac{x_{DDT}}{D_h} = \frac{b_0}{(\sigma-1)^{b_1}} \ln\left[b_2 \left(\frac{D_h}{\delta_f}\right)^{-1} \left(\frac{V_{CJ}}{\sigma s_L}\right)\right]. \quad (4)$$

NLM considers the influence of the most important variables discussed in subsection 3.2 to estimate four constants: a_0, a_1, a_2, and a_3. Note that this expression is general and does not take into account any information regarding the x_{DDT}/D_h trends observed in Figure 4. On the other hand, LM accounts for the logarithmic trend that x_{DDT}/D_h exhibits when plotted as a function of D_h/δ_f and $V_{CJ}/\sigma s_L$. Three constants need being estimated: b_0, b_1, and b_2. The constraint $b_2 > (D_h/\delta_f)(V_{CJ}/\sigma s_L)^{-1}$ was enforced during the

regression so that the argument of the natural logarithm is always greater than unity thereby ensuring that all the $x_{\mathrm{DDT}}/D_{\mathrm{h}}$ estimates are positive; Table 2 lists the fitting results.

Table 2: Models constants.

Model	Eq.	Constants	
		Original	**Updated**
Silvestrini	eq. (1)	$B = 0.0061$ $n = 0.4$ $F = 0.077$	$B' = 0.0057$ $n' = 0.07$ $F' = 0.084$
Dorofeev	eq. (2)	$C = 0.2$ $\kappa = 0.4$ $K = 5.5$ $\zeta = 2.1$ $\xi = 1/3$ $m' = -0.18$	$C' = 0.26$ $\kappa' = 0.13$ $K' = -1.75$ $\zeta' = 0.046$ $\xi' = 1.32$ $m' = 1.46$
NLM	eq. (3)	$a_0 = 184$ $a_1 = 0.82$ $a_2 = 0.11$ $a_3 = 0.29$	
LM	eq. (4)	$b_0 = 50$ $b_1 = 0.7$ $b_2 = 4500$	

Figure 7 shows the fitting with the train, and the evaluation with the test data for a) NLM, and b) LM. Both train and test data are the same sets used in the previous sections to enable a meaningful comparison of the models performance. The LM has a better fit to the training data with an R^2 of 0.78 compared to 0.72 for the NLM. This was also reflected in the performance with the test data, with a R^2 of 0.84 for the LM and 0.74 for the NLM. The prediction of both models is much better than that of the original Dorofeev and Silvestrini, and have higher (LM)/similar (NLM) R^2 values than those obtained with the updated Silvestrini and Dorofeev models. Additionally, note the improvement in the predictions for $x_{\mathrm{DDT}}/D_{\mathrm{h}}$ Exp $<$ 50 when using the LM. This provides evidence of the value of simple data manipulations (e.g., non-linear regressions) to enhance the predictive capabilities of existing models and/or inform the development of new simpler expressions/correlations with comparable or better performance. The most important aspect is the use of large properly curated data sets covering a wide range of experimental conditions, fuels, and geometries to guide the choice of variables that explain the variance of the experimental measurements.

6. Conclusions

A large database is compiled using a comprehensive set of x_{DDT} data for unobstructed channels available in the literature. It comprises an extensive range of experimental conditions and mixtures. The global x_{DDT} trends as a function of D_{h}, ϕ, and p were evaluated. The data shows that x_{DDT} decreases as D_{h} decreases, p increases, and $\phi \to 1$. An analysis of the

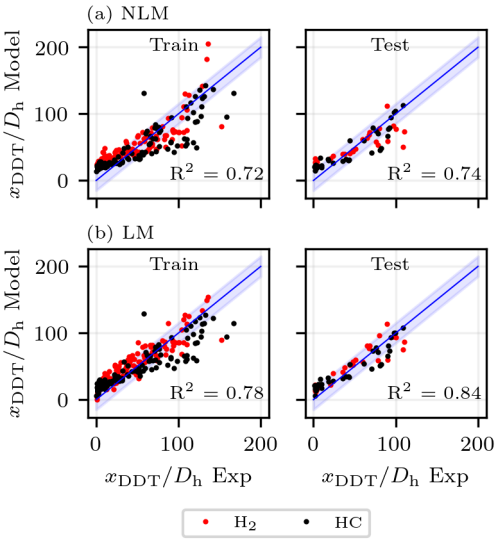

Fig. 7: a) Non-linear (NLM) and b) Logarithmic (LM) models performance for training and test data.

effect of the ratios of fundamental combustion properties on $x_{\mathrm{DDT}}/D_{\mathrm{h}}$ revealed that those that most affect it are $D_{\mathrm{h}}/\delta_{\mathrm{f}}$, $V_{\mathrm{CJ}}/\sigma s_{\mathrm{L}}$ and $\sigma - 1$. The most widely used models for x_{DDT} predictions, i.e., Silvestrini and Dorofeev, were tested against the database performing rather poorly. An update to the models constants was carried out via a non-linear least squares regression using the large database compiled. This resulted in significant improvements in their performance. Finally, two simplified models were proposed. Their predictions are significantly better than those of the original Silvestrini/Dorofeev models and higher (LM)/similar (NLM) to those obtained with the updated models. Future work will include the use of the database to: (i) train a model that will be tested on obstructed channels using an expression that captures the experimental dependence of x_{DDT} as a function of the blockage ratio; (ii) develop $x_{\mathrm{DDT}}/D_{\mathrm{h}}$ models valid for $D_{\mathrm{h}} < 3$ mm and non-unity AR channels.

Acknowledgments

The financial supports from Agence Nationale de la Recherche Program JCJC (FASTD ANR-20-CE05-0011-01), FM Global, Institut PPrime and École Doctoral MIMME are gratefully acknowledged.

References

[1] J. Li, W. Fan, C. Yan, Q. Li, Experimental investigations on detonation initiation in a kerosene-oxygen pulse detonation rocket engine, Combust. Sci. Technol. 181 (3) (2009) 417–432.

[2] M. Silvestrini, B. Genova, G. Parisi, F. L. Trujillo, Flame acceleration and DDT run-up distance for smooth and obstacles filled tubes, J. Loss Prev. Process Ind. 21 (5) (2008) 555–562.

[3] S. B. Dorofeev, Hydrogen flames in tubes: critical run-up distances, Int. J. Hydrog. Energy 34 (14) (2009) 5832–5837.

[4] W. Bartknecht, Brenngas und staubexplosionen forschungsbericht f45, Bundesinstitut Fur Arbeitsschutz (Bifa), Koblenz (1971).

[5] K. Chatrathi, J. E. Going, B. Grandestaff, Flame propagation in industrial scale piping, Process Saf. Prog. 20 (4) (2001) 286–294.

[6] M. Kuznetsov, V. Alekseev, I. Matsukov, S. Dorofeev, DDT in a smooth tube filled with a hydrogen–oxygen mixture, Shock waves 14 (2005) 205–215.

[7] M. Kuznetsov, I. Matsukov, V. Alekseev, W. Breitung, S. Dorofeev, Effect of boundary layer on flame acceleration and DDT, in: Proc. 20th ICDERS, 2005.

[8] M. Kuznetsov, V. Alekseev, A. Bezmelnitsyn, W. Breitung, S. Dorofeev, I. Matsukov, A. Veser, Y. G. Yankin, Report fzka-6328, Karlsruhe: Forschungszentrum Karlsruhe (1999).

[9] M. Kuznetsov et al., Evaluation of structural integrity of typical DN15 tubes under detonation loads, Report Forschungszentrum Karlsruhe (2003).

[10] R. Linds., H. Michels, Deflagration to detonation transitions and strong deflagrations in alkane and alkene air mixtures, Combust. Flame 76 (2) (1989) 169–181.

[11] C. Proust, Gas flame acceleration in long ducts, J. Loss Prev. Process Ind. 36 (2015) 387–393.

[12] G. Thomas, G. Oakley, R. Bambrey, An experimental study of flame acceleration and deflagration to detonation transition in representative process piping, Process Saf. Environ. 88 (2) (2010) 75–90.

[13] R. Blanchard et al., Effect of ignition position on the run-up distance to DDT for hydrogen–air explosions, J. Loss Prev. Process Ind. 24 (2) (2011) 194–199.

[14] Y. Ballossier, F. Virot, J. Melguizo-Gavilanes, Flame acceleration and detonation onset in narrow channels: simultaneous schlieren visualization, Combust. Flame 254 (2023) 112833.

[15] C. Mejia-Botero, F. Virot, J. Melguizo-Gavilanes, CH_4-O_2 flame acceleration morphology: A comparative analysis under different hydrocarbon fuel, channel geometry and scale, Proc. 29th ICDERS (2023).

[16] K. Aizawa et al., Study of detonation initiation in hydrogen/air flow, Shock Waves 18 (2008) 299–305.

[17] B. Baumann et al., On the influence of tube diameter on the development of gaseous detonation, Zeits Elekt Ber der Bun phy Chem 65 (10) (1961) 898–902.

[18] D. Pawel, P. Van Tiggelen, H. Vasatko, H. G. Wagner, Initiation of detonation in various gas mixtures, Combust. Flame 15 (2) (1970) 173–177.

[19] Y. Ballossier, Topologies de l'accélération de flammes d'H_2-O_2-N_2 dans des canaux étroits: de l'allumage jusqu'à la détonation, Ph.D. thesis, ISAE-ENSMA, Poitiers (2021).

[20] J. Melguizo-Gavilanes, Y. Ballossier, L. M. Faria, Experimental and theoretical observations on DDT in smooth narrow channels, Proc. Combust. Inst. 38 (3) (2021) 3497–3503.

[21] T. Tanaka, K. Ishii, T. Tsuboi, A study on shortening of a detonation transition distance, Proc. Symp. Combust. Japanese (2001) 461–462.

[22] L. E. Bollinger, M. C. Fong, R. Edse, Experimental measurements and theoretical analysis of detonation induction distances, ARS J 31 (5) (1961) 588–595.

[23] Z. Yang et al., Experimental investigation on the DDT run-up distance and propagation characteristics of detonation wave in a millimeter-scale spiral channel filled with hydrogen-air mixture, Int. J. Hydrog. Energy (2023).

[24] Z. Yang et al., Experimental study of DDT run-up distance and detonation wave velocity deficit for stoichiometric hydrogen-oxygen mixture in micro spiral channels, Int. J. Hydrog. Energy (2023).

[25] Y. Hsu, Y. Chao, An experimental study on flame acceleration and deflagration-to-detonation transition in narrow tubes, in: Proc. 22th ICDERS, 2009.

[26] J. Huo et al., Deflagration-to-detonation transition and detonation propagation characteristics in a millimetre-scale spiral channel, Exp. Therm. Fluid Sci. 140 (2023) 110773.

[27] P. Urtiew, A. Oppenheim, Experimental observations of the transition to detonation in an explosive gas, Proc. Math. Phys. Eng. 295 (1440) (1966) 13–28.

[28] M. Kuznetsov et al., Experimental study of the preheat zone formation and DDT, Combust. Sci. Technol. 182 (11-12) (2010) 1628–1644.

[29] M. Liberman et al., On the mechanism of the deflagration-to-detonation transition in a H_2-O_2 mixture, J. Exp. Theor. Phys. 111 (2010) 684–698.

[30] R. Lindstedt, H. Michels, Deflagration to detonation transition in mixtures of alkane LNG/LPG constituents with O_2-N_2, Combust. Flame 72 (1) (1988) 63–72.

[31] Y. Zhao, Y. Zhang, Large eddy simulation investigation of flame acceleration and DDT of CH_4-air mixture in rectangular channel, Eng. Rep. 5 (3) (2023) e12574.

[32] H. Steen, K. Schampel, Experimental investigations on the run-up distance of gaseous detonations in large pipes, in: 4th Int. Symp, Loss Prev. Saf. Prom. Process Ind., Vol. 82, 1983, pp. E23–33.

[33] M. Wu et al., Flame acceleration and the transition to detonation of stoichiometric C_2H_4/O_2 in microscale tubes, Proc. Combust. Inst. 31 (2) (2007) 2429–2436.

[34] M. Wu et al., Transmission of near-limit detonation wave through a planar sudden expansion in a narrow channel, Combust. Flame 159 (11) (2012) 3414–3422.

[35] C.-Y. Wang, J.-K. Wang, M.-H. Wu, Visualization and parametric study of reaction propagation in meso-scale tubes, in: ASME, Vol. 43765, 2009, pp. 265–271.

[36] J. Li, P. Zhang, L. Yuan, Z. Pan, Y. Zhu, Flame propagation and detonation initiation distance of ethylene/oxygen in narrow gap, Appl. Therm. Eng. 110 (2017) 1274–1282.

[37] J. Finigan et al., Deflagration-to-detonation transition via the distributed photo ignition of carbon nanotubes suspended in fuel/oxidizer mixtures, Combust. Flame 159 (3) (2012) 1314–1320.

[38] F. Pintgen, Z. Liang, J. Shepherd, Structural response of tubes to deflagration-to-detonation transition, in: Proc. 21th ICDERS, 2007, pp. 23–27.

[39] M. Liberman et al., Deflagration-to-detonation transition in highly reactive combustible mixtures, Acta Astronaut. 67 (7-8) (2010) 688–701.

[40] J. Li, W.-H. Lai, K. Chung, Tube diameter effect on deflagration-to-detonation transition of propane–oxygen mixtures, Shock waves 16 (2006) 109–117.

[41] Z. Pan, Z. Zhang, P. Zhang, Effects of a significant boundary layer on the flame acceleration and transition to detonation in millimeter-scale tubes, Aerosp. Sci. Technol. 126 (2022) 107533.

[42] H.-W. Ssu, M.-H. Wu, Formation and characteristics of composite reaction–shock clusters in narrow channels, Proc. Combust. Inst. 38 (3) (2021) 3473–3480.

[43] F. Pedregosa et al., Scikit-learn: Machine learning in Python, J. Mach. Learn. Res. 12 (2011) 2825–2830.